High-Density Field-Reversed Configuration Plasma for Magnetized Target Fusion

Shouyin Zhang, Glen A. Wurden, *Senior Member, IEEE*, Thomas P. Intrator, *Member, IEEE*, Edward L. Ruden, *Member, IEEE*, William J. Waganaar, Chris T. Grabowski, Richard M. Renneke, and James H. Degnan, *Senior Member, IEEE*

***Abstract*—Field Reversed Theta Pinch technology is employed with programmed cusp fields at the theta coil ends to form high-density field-reversed configuration (FRC) plasmas. The well-formed FRC plasmas have volume-averaged density of 2-4×10^{22} m^{-3}, total temperature (T_e+T_i) of 300-500 eV, and plasma lifetime between 10-20 μs in 50 mTorr to 70 mTorr of deuterium static gas fill. The achieved FRC parameters are very close to the desired target plasma requirements for Magnetized Target Fusion.**

***Index Terms*—Field-reversed configuration, Magnetized Target Fusion, Plasmas, plasma generation, plasma pinch, plasma confinement, plasma measurements, fusion reactors**

Manuscript received September 8, 2005. Revised January 16, 2006. This work was supported by the Department of Energy—Office of Fusion Energy Sciences under Contract W-7405-ENG-36.

Shouyin Zhang is currently with the Department of Physics at University of Wisconsin-Madison, 1150 University Avenue, Madison, WI 53706, USA; e-mail: sy_zhang66@hotmail.com; szhang9@wisc.edu. He was a Postdoctoral Research Associate at Los Alamos National Laboratory, Los Alamos, NM 87545, USA.

Glen A. Wurden, Thomas P. Intrator, William J. Waganaar, and Richard M. Renneke are with the P-24 Plasma Physics Group, Los Alamos National Laboratory, Los Alamos, NM 87545, USA.

Edward L. Ruden and James H. Degnan are with the Air Force Research Laboratory, Albuquerque, NM 87117, USA.

Chris T. Grabowski is with the Science Applications International Corporation, Albuquerque, NM 87106, USA; he is contracted with the Air Force Research Laboratory.

I. INTRODUCTION

Approaches to plasma fusion research are usually categorized as either Magnetic confinement Fusion Energy (MFE) [1] or Inertial Confinement Fusion (ICF) [2]. At Los Alamos National Laboratory, we are exploring the concept of Magnetized Target Fusion (MTF) [3], where the plasma density and lifetime lie between those of MFE and ICF.

A number of plasma configurations and plasma compression schemes have been proposed for MTF [4, 5]. We have chosen the field-reversed configuration (FRC) as the target plasma with a solid cylindrical liner ("pusher") to adiabatically compress the FRC in the FRC-MTF scheme [6, 7].

The first phase of the approach is to reliably produce a target FRC plasma with density of 10^{23} m^{-3}, total temperature in the range of 150 - 300 eV, and a lifetime of approximately 20 μs. An integrated experiment to implode (compress) the target FRC plasma with a liner is planned on the Shiva-Star facility of Air Force Research Laboratory in Albuquerque, New Mexico [8].

II. THE FIELD-REVERSED CONFIGURATION EXPERIMENTS AT LOS ALAMOS NATIONAL LABORATORY

Field-Reversed Theta Pinch (FRTP) technology is employed with programmed cusp fields at the theta coil ends to achieve non-tearing field line reconnection during FRC formation [9]. Fig. 1 schematically shows the field-reversed configuration

experiment with a Liner (FRX-L) at Los Alamos National Laboratory. The single-turn aluminum theta coil of 36 cm in length is segmented into four segments (A, B, C, and D) with 1 cm slots between the segments for laser and optic diagnostic access. The internal diameter of theta coil is 12.4 cm. The plasma vessel is a fused quartz tube of 10.6 cm internal diameter, concentric with theta coil bore hole. The peak strength of the main compression field is about 30 kG, and the net bias field in the middle of theta coil confinement region is about 2 kG. Instead of having notches at theta coil ends to provide mirror field at theta coil ends to localize the FRC during formation [10], the FRX-L theta coil sections are bored with a constant diameter. The cusp field (which is in a direction opposite to that of the bias field) is in the same direction as main compression field, and thus acts as a weak mirror field at theta coil ends after main compression field is initiated.

Arrays of tiny magnetic coil probes (measuring external magnetic fields B_e) distributed along axis and four flux loops monitors the FRC excluded flux radius profile $r_s(t,z)$ [11]. Eight channels of side-on helium-neon laser interferometer measure the plasma line integrated density $\bar{n}_e = \int < n_e > dl$ at the midplane of the theta coil along different chords. Optical multi-channel analyzer spectroscopy and monochromators monitor visible impurity visible lines emitted from the plasma. A framing camera takes end-on visible light pictures of plasmas every microsecond up to eight frames that help understanding the effects of asymmetry structures existing in the pre-ionization plasma phase on FRC formation.

In 2002, FRX-L produced some FRC plasmas with basic diagnostics to show the FRC properties; in 2003, FRX-L demonstrated that high-density, long-lived FRC plasmas could be formed [12]. In early 2004, FRX-L achieved high reproducibility in forming the high-density, long-lived FRCs [13]; and in 2005, new crowbar switch installation reduced the main field modulation. Preliminary results showed improved plasma density and temperature properties. Currently, design of an integrated experiment of FRC-MTF at Shiva-Star facility is in progress.

III. EVOLUTION OF THE HIGH-DENSITY FRC PLASMA

Fig. 2 shows some of the main parameters of a typical well-confined high-density FRC plasma formed at 50 mTorr of deuterium static gas fill. The plasma has volume-averaged density of 2 - 4×10^{22} m^{-3} measured by the laser interferometry and separatrix radius diagnostics, the total temperature (T_e+T_i) of 300-500 eV is derived as a result of radial pressure equilibrium, and the plasma lifetime is about 15 μs. These parameters are very close to the desired parameters of a target plasma for MTF, and can be nicely reproduced shot to shot within windows of identified engineering controllable parameter settings.

The FRC undergoes radial compression between 24.8 - 25.7 μs and axial contraction around 26.2 μs, then it enters into the equilibrium phase until it is terminated by the development of the n = 2 rotational instability. The FRC maintains high density at 4×10^{22} m^{-3} and high temperature around 500 eV for about 1 μs after it is formed, then

the parameters dropped to their halves as the plasma expanded in volume in response to the external confinement field (the main field) reduction due to the poor performance of crowbar switch installations. With eight channels interferometer measurements of line-integrated densities, the FRC is clearly seen rotating like a rigid-body as the n = 2 rotational instability develops. The rotation angular frequency is about $(1.5 – 2.5) \times 10^6$ Rad/Sec. As an example, in Fig. 2(b), the off-center line-integrated density signal (ch3) is in opposite phase with the center channel (ch1) when n = 2 rotational instability developed into observable stage at the density signals (after 33 μs). The FRC stable time (τ_s, it is also called FRC stable period [14]) is thus experimentally determined in FRX-L as the time interval between the peak density (axial contraction) and the observable opposite signal phases shown in the center (ch1) and off-center line-density channels (ch3 to ch8).

As in previous FRC studies [14], n = 2 rotational instability terminated most of the FRCs in FRX-L, therefore, the dealing with n = 2 instability is a very important issue in the proposed MTF scheme. Preliminary analysis does show unfavorable scaling of the growth rate of the instability when an FRC with n = 2 development is compressed. A simple picture of that is, the rotational angular frequency will get faster and faster as the FRC's separatrix radius is decreasing due to angular momentum conservation during compression, meanwhile the particle losses have always been kicking off the plasma rotation.

For the application of FRC to MTF, we adopted a simple approach to mitigate the problem. The idea is just to form adequately long-lived FRC plasma and subsequently

translate and compress the target plasma quickly enough so that the FRC could not gain enough angular momentum to develop catastrophic deformation. If an FRC is formed in 3 μs, it is to be translated for ~60 cm at Alfven velocity (~10 cm/μs) and compressed at speed of ~cm/μs in radial direction, the stable time of the target FRC is desired to be around ~12 μs. The extrapolation of existing FRC scaling laws indeed suggest that such stable time is possible in the interested density regime [13, 15, 16]. Our current record FRC stable time in FRX-L is ~10.5 μs after a major effort of improving the main field performance declared a success (shown in Section V).

The FRC shown in Fig.2 preserves good initial flux and particle trapping efficiencies. The ratio of the lift-off flux to the net bias field is 0.84, and the FRC initially traps 85% of all the particles inside the theta coil confinement region. The measured flux confinement time τ_Φ is between 20-40 μs for the well confined FRCs in FRX-L. As a comparison, in a simple model, the flux confinement time τ_Φ of the FRC is estimated by the perpendicular diffusion coefficient $D_\perp$ calculated from the classical transverse Spitzer resistivity $\eta_\perp$ and the directly measured FRC separatrix radius r_s [17]. $\tau_\Phi = r_s^2 / 16 D_\perp \approx 120 \mu s$ is obtained for the described FRC plasma in Fig.2 assuming electron temperature T_e to be half of the deduced plasma total temperature. That is to say the FRC's flux decay diffusivity anomaly factor is 3-6 over the classical one, which is in the range seen by most of the previous FRC experiments [14]. So far, all the results in FRX-L confirmed that the FRCs still observe the empirical scaling laws obtained from

previous experiments in fill pressure mostly less than 20 mTorr; the results also encourage us to continue the effort to form long-lived FRCs as target plasmas for MTF.

However, researchers at University of Washington recently showed a method to form low density FRC plasma at lifetime several times longer than the prediction of scaling laws; the method might worth exploring to see if it might be able to extend to FRC formation in higher density regimes [18]. Other considerations to make use of the well-demonstrated technique of multipole field stabilization to control the n = 2 rotational instability during translation and compression [19] are also under seriously scrutinizing, although the application of the technique if possible would unavoidably introduce much more complexity into the FRC-MTF scheme.

IV. ACHIEVING REPRODUCIBLE FRC PLASMAS FOR MTF

In an integrated MTF experiment, high-density FRC plasma is formed and translated quickly into an Aluminum liner; the target plasma and the liner are then compressed adiabatically in several micro-seconds. The liner and its surrounding structures are to be destructed during each implosion experiment although there may not be desired target plasma inside the liner. The recovery and preparation for a next implosion is both time-consuming and costly. It is thus obvious that the reproducibility of FRC plasma formation plays a key role in the success of an integrated FRC-MTF experiment. Unfortunately, previous studies have shown that the reproducibility of FRC

formation by FRTP is usually poor [14]. Therefore, considerable efforts are made to improve the formation reproducibility of high-density and long-lived FRCs in FRX-L.

Several key factors such as impurity level, timing, and cusp point locations at theta coil ends have been identified in FRX-L to improve the FRC parameter reproducibility in consecutive discharges. Fig. 3 shows the dynamics of a pre-ionization (PI) plasma. The visible light pictures were taken by a framing camera at 1 μs intervals with exposure time of 200 ns. After the working gas was broken down by a quick ringing PI field at 2.7 μs, a plasma annulus was formed. The plasma annulus then underwent cycles of compression and expansion along with the ringing of PI field cycles. Asymmetry structures (flute mode) of Rayleigh-Taylor instability developed after the first compression on the plasma annulus. The asymmetries died away after 4-5 PI ringing cycles. Discharge statistics showed that it has much better chance to obtain a well-confined FRC plasma if there are no asymmetry structures presented in the PI plasma annulus when the main field is switched on; and major plasma parameters are usually also higher than the FRCs formed with the presence of the asymmetries. As an example, Fig. 4 shows the mean trapped poloidal fluxes in FRCs during their equilibrium at different main field switch-on time for well-confined FRC plasmas. Error bars represent the standard deviations from shot to shot at the same timing. The trapped fluxes are higher around 7 μs and 24 μs, where the asymmetry structures either have not developed yet or they have died away. FRC plasmas trapped the highest poloidal fluxes with minimum shot-to-shot deviations during the narrow time window around 24 μs, which indicated the high reproducibility of the parameter in the shots.

Fig. 5 shows the relative intensities of oxygen spectral lines in PI plasmas along with the charging voltage of PI capacitor banks. The oxygen level in PI plasma is an indication of the interaction between PI plasma annulus and the quartz tube wall. Applying minimum PI ringing voltage can effectively reduce the plasma-wall interactions that release impurities from the quartz tube wall material. It is observed that high amounts of impurities in PI plasma usually lead to escape of FRC plasmas from the theta coil confinement region.

V. IMPROVING FRC PERFORMANCE

Due to the large inductance in the original crowbar switch, the crowbarred main field experienced strong amplitude modulation of about 50%, which tailored the FRC plasma parameters through its lifetime. Shown in Fig. 6, the contour of the excluded flux radii indicates the expansion and shrinking of FRC volume along with the main field modulation. It also shows the axial shifting of the FRC geometric center. The geometric centroid was about 0.7 cm west from theta coil midplane just after axial contraction and it drifted west to 1.7 cm during the middle of equilibrium phase. The moving speed is about 0.6 cm/μs, which is several percent of the local Alfven velocity. In shots of poorly confined FRCs, plasmas often escaped from either ends of the theta coil at speeds up to 10% of the local Alfven velocity.

A new, lower inductance crowbar switch design has been installed to reduce crowbarred main field modulation. Initial tests show that the modulation is reduced from

original 50% to 25% now. Should the improvement enable the existing theta coil to house the FRC plasma, the high-density, high temperature feature presented immediately after the FRC axial contraction will last through the whole FRC lifetime. Fig. 7 shows the comparison of the measured external fields between new crowbar design (solid line) and previous design (dashed line). The ringing frequency of the crowbarred main field almost doubled; the average field strength after crowbarred increased by 5 kG.

Fig. 8 shows the temporal evolution of some of the key parameters in a well-confined FRC plasma with the new crowbar switch design. As anticipated, the density and temperature of the FRC remained flat and high during the equilibrium, with values at 3.7×10^{22} m^{-3} and 370 eV. The excluded flux radius contour (Fig. 9) confirmed that the FRC was completely confined inside theta coil region as expected. Recently, in another shot (Fig. 10), a long-lived FRC plasma was obtained at 70 mTorr filled gas pressure. The FRC's stable time reached 10.5 μs in comparison to that of 7 μs for typical well-formed FRCs with old crowbar switch installation. More data are yet to come in the scheduled experimental campaigns.

VI. CONCLUSION

High-density, long-lived FRC plasmas have been formed in FRX-L device at Los Alamos National Laboratory. The density achieved is about one-third of that of the required target plasma; the temperature is in the range of the requirement, and the

lifetime is close to the target plasma. With the identification of the key factors that govern the FRC formation in FRX-L, essential FRC parameters can be nicely reproduced shot-to-shot to meet the expectation of applying FRC as target plasma for MTF.

ACKNOWLEDGMENT

The authors would like to thank D. Begay, E. M. Tejero, R. Aragonez, and E. Mignardot for their timely support to the project.

REFERENCES

1. J. Wesson, Tokamaks, 2nd ed. Oxford: Clarendon, 2004, pp.1-27.
2. J. Lindl, "Development of the indirect-drive approach to inertial confinement fusion and the target physics basis for ignition and gain," *Phys. Plasma,* vol. 2**,** no. 11, pp. 3933-4024, 1995.
3. R. C. Kirkpatrick, I. R. Lindemuth, and M. S. Ward, "Magnetized target fusion: an overview," *Fusion Technol.,* vol. 27**,** pp. 201-214, 1995.
4. I. R. Lindemuth, R. E. Reinovsky, R. E. Chrien *et al.*, "Target plasma formation for magnetic compression/magnetized target fusion," *Phys. Rev. Lett.,* Vol. 75, no. 10, pp. 1953-1956, 1995.

5. A. J. Kemp, M. M. Basko, and J. Meyer-ter-vehn, "Implosion and ignition of magnetized cylindrical targets driven by heavy-ion beams," *Nucl. Fusion*, vol. 43, pp. 16-24, 2003.
6. R. E. Siemon, R I. Lindemuth., and K. F. Schoenberg, "Why MTF is a low cost path to fusion," *Comments Plasma Phys. Control. Fusion*, vol. 18, no. 6, pp. 363-386, 1999.
7. G.A. Wurden, K. F. Schoenberg, R. E. Siemon *et al.*, "Magnetized target fusion: a burning FRC plasma in an imploded metal can," *Journal Plasma Fusion Res. Series*, vol. 2, pp. 238-241, 1999.
8. J. H. Degnan, J. M. Taccetti, T. Cavazos *et al.*, "Implosion of solid liner for compression of field reversed configuration," *IEEE Trans. on Plasma Science*, vol. 29, no. 1, pp. 93-98, 2001.
9. J. M. Taccetti, T. P. Intrator, G. A. Wurden *et al.*, "FRX-L: A field-reversed configuration plasma injector for magnetized target fusion," *Rev. Sci. Instrum.*, vol. 74, no. 10, pp. 4314-4323, 2003.
10. A. L. Hoffman, R. D. Milroy, J. T. Slough, and L. C. Steinhauer, "Formation of field-reversed configurations using scalable low-voltage technology," *Fusion Technol.*, vol. 9, pp. 48-57, Jan. 1986.
11. S. Y. Zhang, E.M. Tejero, J.M. Taccetti, G.A. Wurden, T.P. Intrator, W.J. Waganaar, R, Perkins, "Separatrix radius measurement of field-reversed configuration plasma in FRX-L," *Rev. Sci. Instrum.*, vol. 75, no.10, pp. 4289-4292, 2004.

12. T. Intrator, S. Y. Zhang, J. H. Degnan, *et al.*, "A high density field reversed configuration (FRC) target for magnetized target fusion: First internal profile measurements of a high density FRC," *Phys. Plasmas*, vol. 11, no. 5, pp. 2580-2585, 2004.

13. Shouyin Zhang, T. P. Intrator, G. A. Wurden, W. J. Waganaar, C. Grabowski, E. L. Ruden, J. M. Taccetti, and R. Renneke, "Confinement analyses of the high-density field-reversed configuration plasma in the field-reversed configuration experiment with a liner," *Phys. Plasmas*, vol. 12, 052513 pp.1-8, 2005.

14. M. Tuszewski, "Field reversed configurations," *Nucl. Fusion*, vol. 28, no. 11, pp. 2033-2092, 1988.

15. J. Lipson, W. T. Armstrong, J. C. Cochrane, K. F. McKenna, E. G. Sherwood, and M. Tuszewski, "Scaling studies in field reversal experiments," *Appl. Phys. Lett.* vol. 39, no. 1, pp. 43-45, July 1981.

16. M. Tuszewski, G. A. Barnes, R. E. Chrien, W. N. Hugrass, D. J. Rej, R. E. Siemon, and B. Wright, "The origin of the rotation in field-reversed configurations," *Phys. Fluids*, vol. 31, no. 4, pp. 946-948, Apr. 1988.

17. A. L. Hoffman and J. T. Slough, "Flux, energy, and particle lifetime measurements for well formed field reversed configurations," *Nucl. Fusion*, vol. 26, no.12, pp. 1693-1702, 1986.

18. H.Y. Guo, A. L. Hoffman, L. C. Steinhauer, and K. E. Miller, "Observations of improved stability and confinement in a high-β_self-organized spherical-torus-like field-reversed configuration, vol. 95, Phys. Rev. Lett., 175001, Oct. 21, 2005.

19. S. Ohi, T. Minato, Y. Kawakami, M. Taniyo, S. Okada, Y. Ito *et al.*, "Quadrupole stabilization of n = 2 rotational insatability of a field-reversed theta-pinch plasma," Phys. Rev. Lett., vol. 51, no. 12**,** pp. 1042-1045, Sept. 19, 1983.

Figure Captions

Fig. 1. The schematic drawing of FRX-L. Shown in the figure are theta coil segments (labeled A, B, C, D), cusp coil and stainless steel flux excluder plates beyond theta coil ends, fused quartz tube and some diagnostics.

Fig. 2. Temporal evolution of the plasma parameters of a well-confined high-density FRC plasma. (a) measured external magnetic field at midplane, (b) line integrated density measurements at center channel (ch1, impact parameter at 0 cm) and one of the off-center channels (ch3, impact parameter at 1.9 cm), indicating the evolution of rotational instability as well as FRC stable time τ_s, (c) volume-averaged density, (d) total temperature, (e) normalized separatrix radius r_s by theta coil radius r_c=6.2cm at midplane, and (f) the trapped poloidal flux.

Fig. 3. Development of asymmetry structures in pre-ionization (PI) plasma annulus due to Rayleigh-Taylor instability. Photographs were taken by IMACON 775 framing camera at 1 μs interval from end-on viewing. The outer bright rings are the reflections of quartz tube wall lit by plasma light.

Fig. 4. Statistics on trapped poloidal fluxes in FRC plasmas at different main field switch-on timing. Error bars show deviations from shot-to-shot; no error bar means only one shot is available in the data.

Fig. 5. Relative intensity of Oxygen spectral lines along with the scanning of charging voltage of PI capacitor banks at wavelengths of λ= 464.64 nm, 470.40 nm, 493.20 nm

and 494.48 nm measured by Optical Multi-channel Analyzer (OMA) spectroscope. Two shots at the same plasma conditions were fired.

Fig. 6. Contour of the separatrix radii (approximated by the excluded flux radius measurement) indicating the movement of FRC geometric centroid and the volume expansion with the modulation of the main field. The values marked on the curves are separatrix radii in cm.

Fig. 7. Reduction in crowbarred main field modulation for upgraded crowbar switch design (indicated as new switch) over its previous design (indicated as old switch).

Fig. 8. Temporal evolution of the plasma parameters of a well-confined high density FRC plasma formed with upgraded crowbar switch installation. (a) measured external magnetic field at midplane, (b) volume-averaged density, (c) total temperature, (d) normalized separatrix radius at midplane, and (e) the trapped poloidal flux.

Fig. 9. Contour of the separatrix radii measured in shot 3684 confirmed that FRC plasma was completely confined inside the theta coil region. The values marked on the curves are separatrix radii in cm.

Fig. 10. Comparison of the FRC stable time (τ_s) measured by line-integrated density in FRCs formed with new crowbar switch installation (solid line, shot 3768) to a typical shot with old crowbar switch design (dashed line, shot 3074).

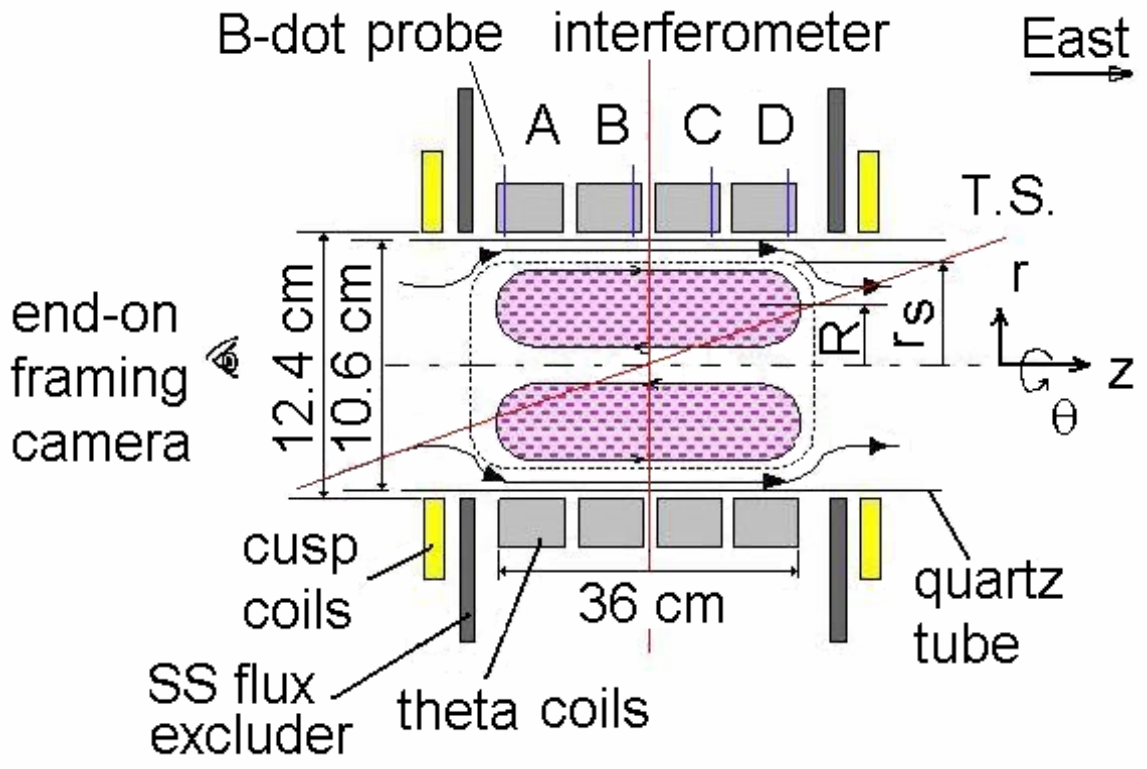

Fig. 1. The schematic drawing of FRX-L. Shown in the figure are theta coil segments (labeled A, B, C, D), cusp coil and stainless steel flux excluder plates beyond theta coil ends, fused quartz tube and some diagnostics.

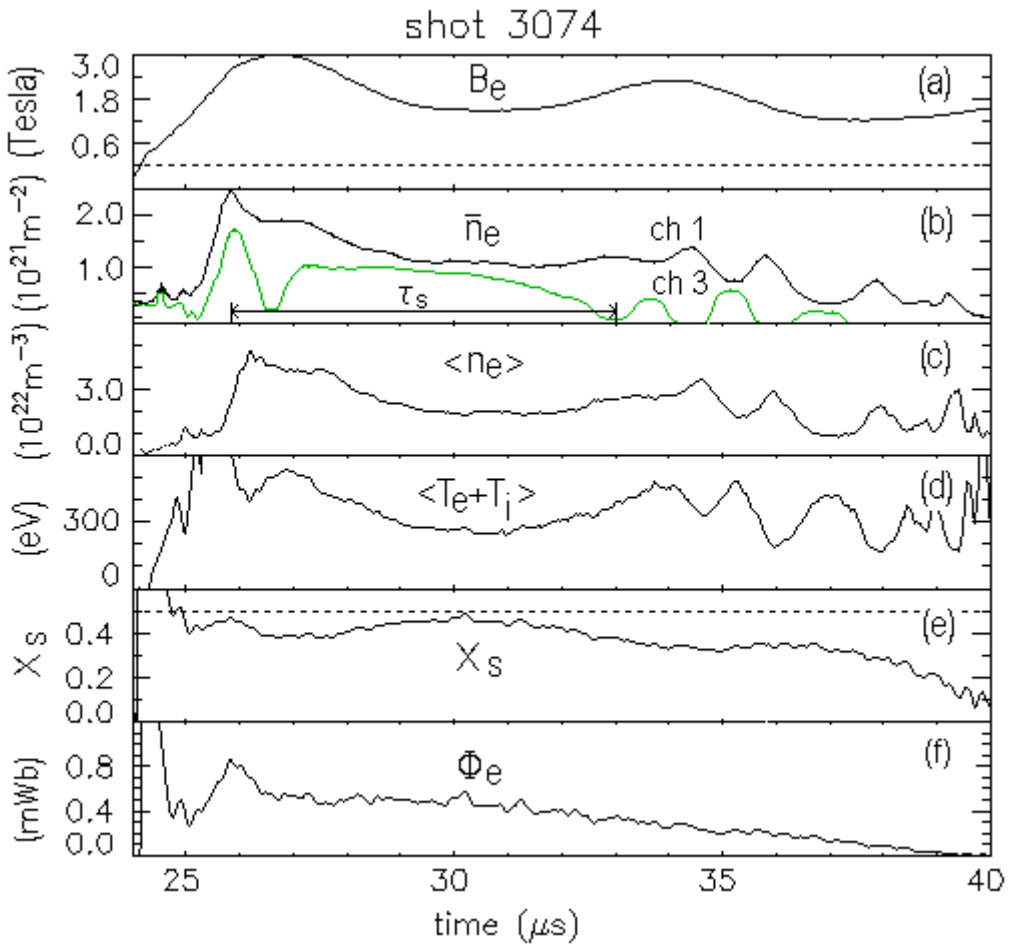

Fig. 2. Temporal evolution of the plasma parameters of a well-confined high-density FRC plasma. (a) measured external magnetic field at midplane, (b) line integrated density measurements at center channel (ch1, impact parameter at 0 cm) and one of the off-center channels (ch3, impact parameter at 1.9 cm), indicating the evolution of rotational instability as well as FRC stable time τ_s, (c) volume-averaged density, (d) total temperature, (e) normalized separatrix radius r_s by theta coil radius r_c=6.2cm at midplane, and (f) the trapped poloidal flux.

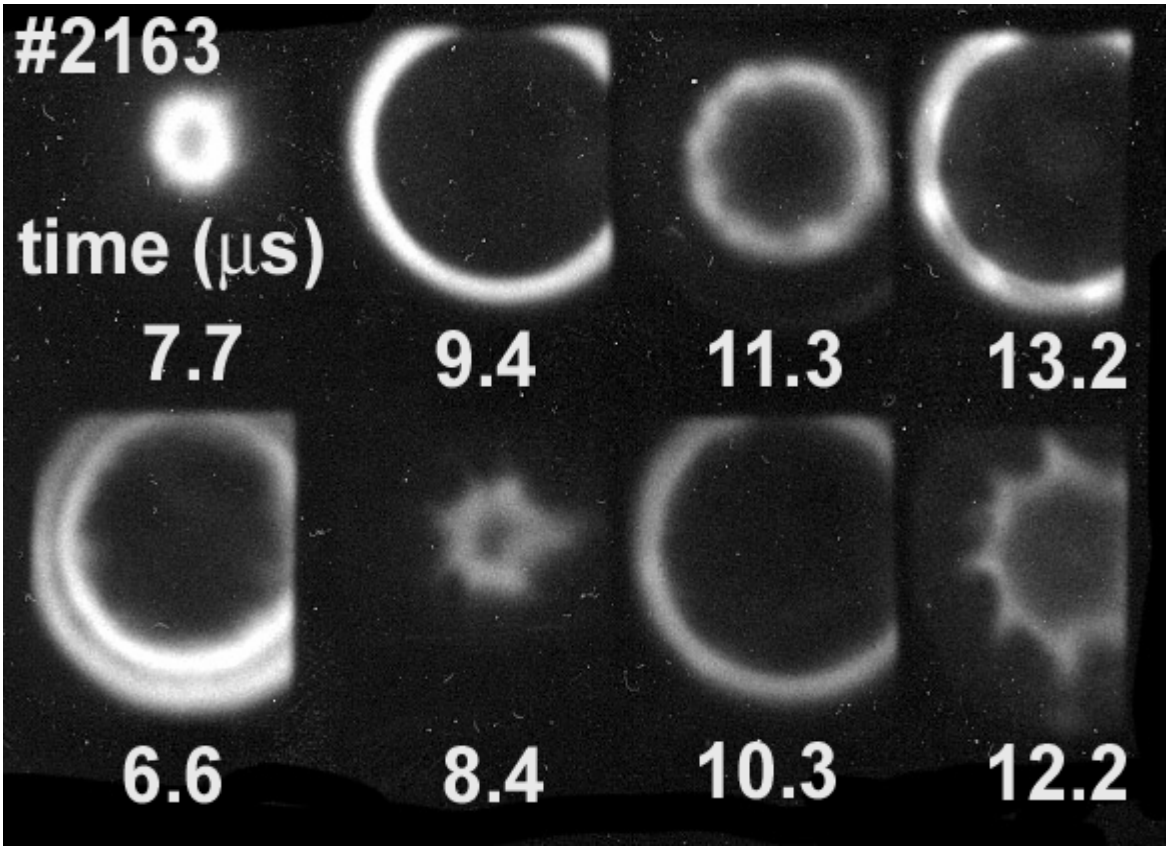

Fig. 3. Development of asymmetry structures in pre-ionization (PI) plasma annulus due to Rayleigh-Taylor instability. Photographs were taken by IMACON 775 framing camera at 1 μs interval from end-on viewing. The outer bright rings are the reflections of quartz tube wall lit by plasma light.

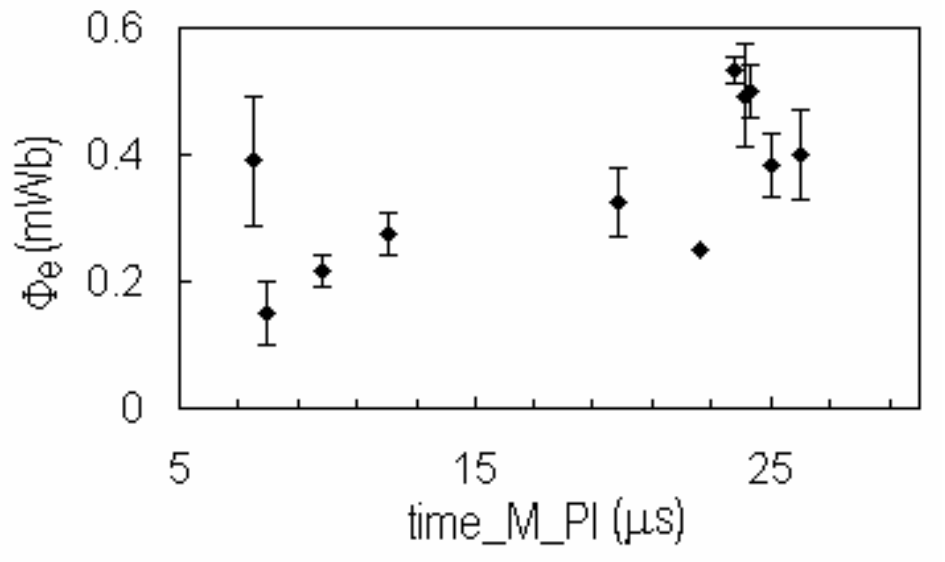

Fig. 4. Statistics on trapped poloidal fluxes in FRC plasmas at different main field switch-on timing. Error bars show deviations from shot-to-shot; no error bar means only one shot is available in the data.

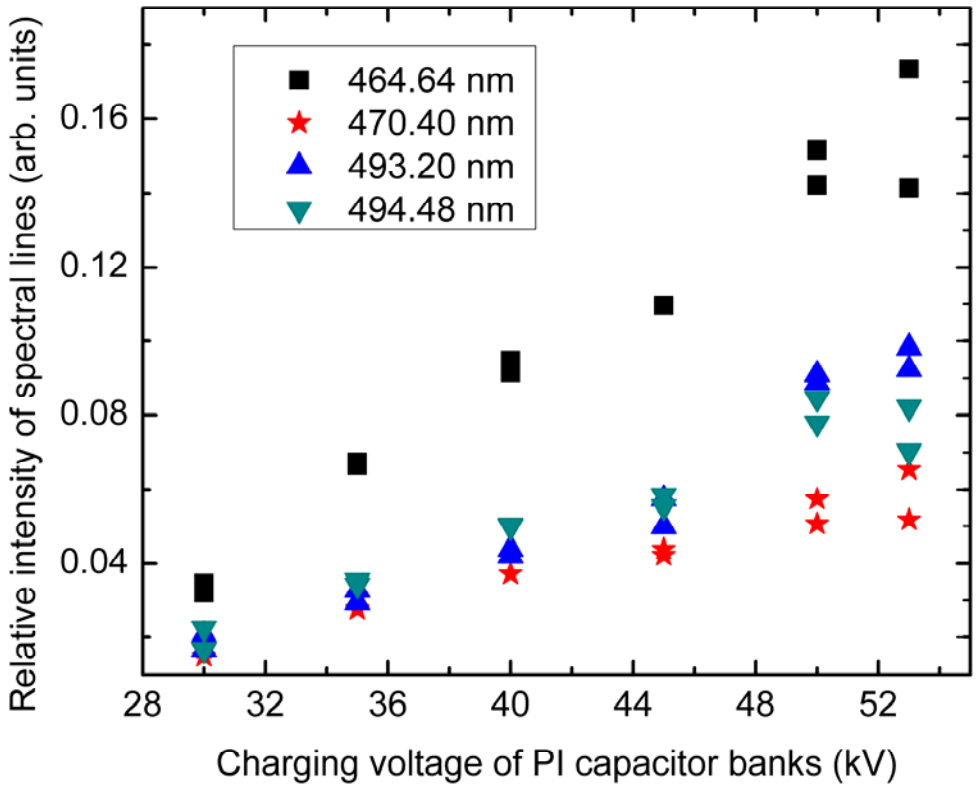

Fig. 5. Relative intensity of Oxygen spectral lines along with the scanning of charging voltage of PI capacitor banks at wavelengths of λ= 464.64 nm, 470.40 nm, 493.20 nm and 494.48 nm measured by Optical Multi-channel Analyzer (OMA) spectroscope. Two shots at the same plasma conditions were fired.

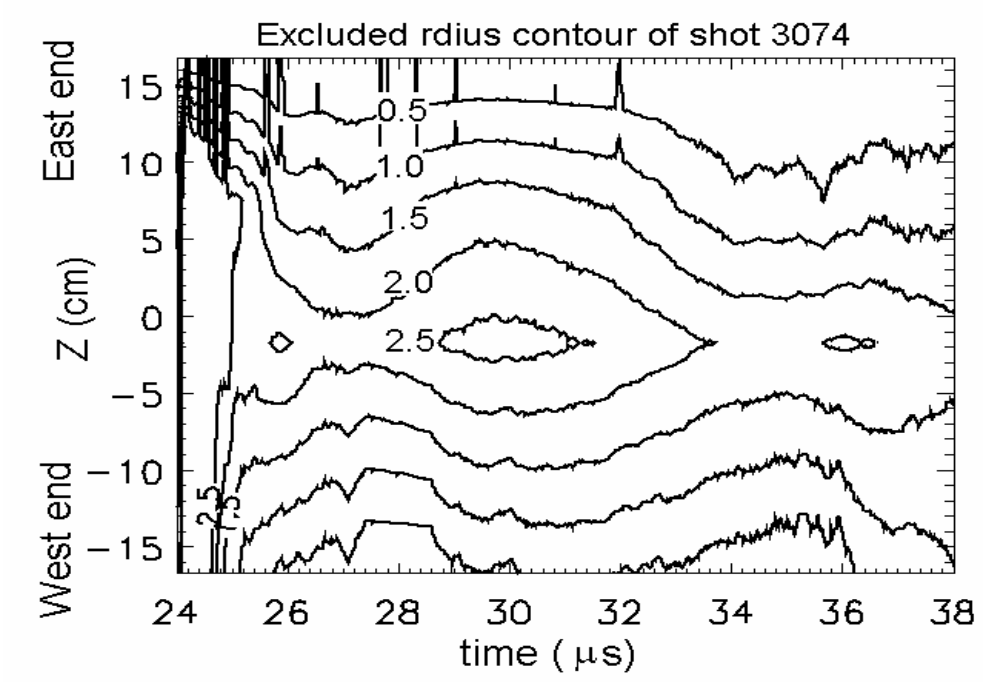

Fig. 6. Contour of the separatrix radii (approximated by the excluded flux radius measurement) indicating the movement of FRC geometric centroid and the volume expansion with the modulation of the main field. The values marked on the curves are separatrix radii in cm.

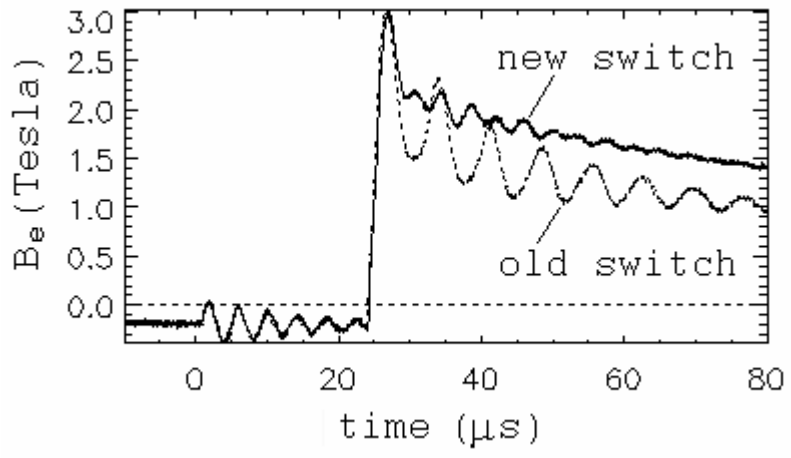

Fig. 7. Reduction in crowbarred main field modulation for upgraded crowbar switch design (indicated as new switch) over its previous design (indicated as old switch).

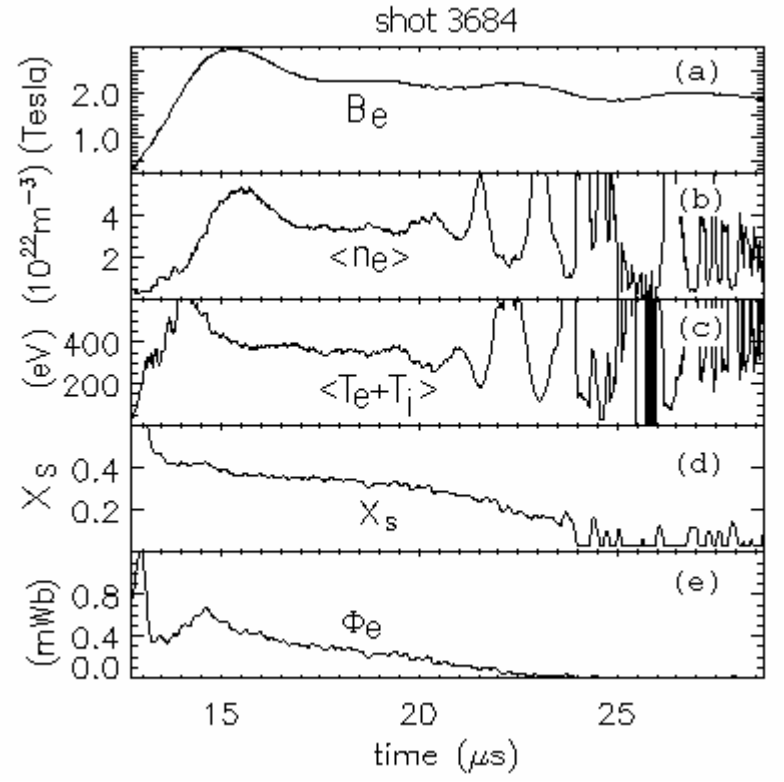

Fig. 8. Temporal evolution of the plasma parameters of a well-confined high density FRC plasma formed with upgraded crowbar switch installation. (a) measured external magnetic field at midplane, (b) volume-averaged density, (c) total temperature, (d) normalized separatrix radius at midplane, and (e) the trapped poloidal flux.

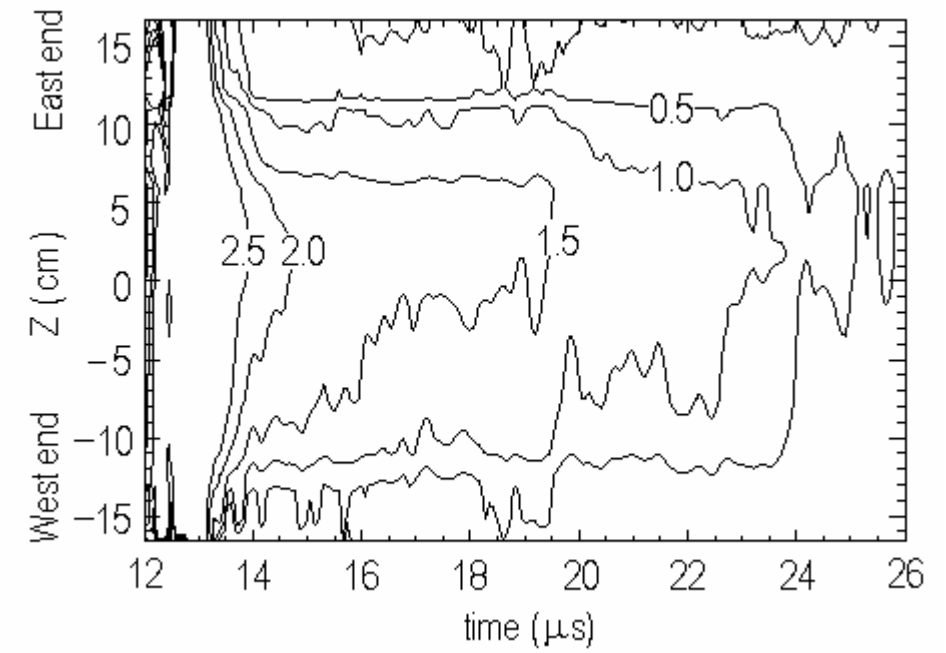

Fig. 9. Contour of the separatrix radii measured in shot 3684 confirmed that FRC plasma was completely confined inside the theta coil region. The values marked on the curves are separatrix radii in cm.

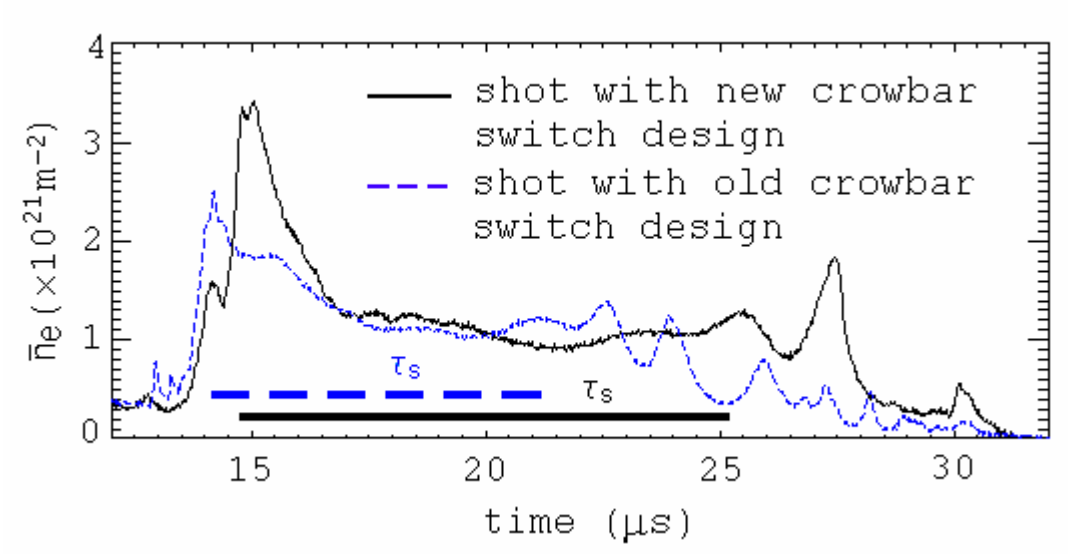

Fig. 10. Comparison of the FRC stable time (τ_s) measured by line-integrated density in FRCs formed with new crowbar switch installation (solid line, shot 3768) to a typical shot with old crowbar switch design (dashed line, shot 3074).